Mass-movement and flood-induced deposits in Lake Ledro, southern Alps, Italy: implications for Holocene palaeohydrology and natural hazards

A. Simonneau[1,*], E. Chapron[1], B. Vannière[2], S. B. Wirth[3], A. Gilli[3], C. Di Giovanni[1], F. S. Anselmetti[4,6], M. Desmet[1,5], and M. Magny[2]

[1]ISTO, UMR7327, CNRS; Univ Orléans; BRGM, 1A rue de la Férollerie, 45071 Orléans Cedex 2, France
[2]Laboratoire de Chrono-Environnement, UMR6249 CNRS, UFR des Sciences et Techniques, 16 route de Gray, 25030 Besançon, France
[3]Geological Institute, ETH Zurich, Sonneggstrasse 5, 8092 Zurich, Switzerland
[4]Eawag, Department of Surface Waters, Überlandstrasse 133, 8600 Dübendorf, Switzerland
[5]GéoHydrosystème COntinentaux, E.A. 6293 GéHCO, Université F. Rabelais de Tours, Département Géosciences-environnement, Faculté des Sciences et Techniques, Parc de Grandmont, 37200 Tours, France
[6]Institute of Geological Sciences and Oeschger Centre for Climate Change Research, University of Bern, Baltzerstrasse 1–3, 3012 Bern, Switzerland
[*]present address: GEODE, UMR5602, CNRS; Université de Toulouse 2, Allée A. Machado, 31058 Toulouse Cedex, France

Correspondence to: A. Simonneau (anaele.simonneau@univ-tlse2.fr)

Abstract. High-resolution seismic profiles and sediment cores from Lake Ledro combined with soil and riverbed samples from the lake's catchment area are used to assess the recurrence of natural hazards (earthquakes and flood events) in the southern Italian Alps during the Holocene. Two well-developed deltas and a flat central basin are identified on seismic profiles in Lake Ledro. Lake sediments have been finely laminated in the basin since 9000 cal. yr BP and frequently interrupted by two types of sedimentary events (SEs): light-coloured massive layers and dark-coloured graded beds. Optical analysis (quantitative organic petrography) of the organic matter present in soil, riverbed and lacustrine samples together with lake sediment bulk density and grain-size analysis illustrate that light-coloured layers consist of a mixture of lacustrine sediments and mainly contain algal particles similar to the ones observed in background sediments. Light-coloured layers thicker than 1.5 cm in the main basin of Lake Ledro are synchronous to numerous coeval mass-wasting deposits remoulding the slopes of the basin. They are interpreted as subaquatic mass-movements triggered by historical and pre-historical regional earthquakes

dated to AD 2005, AD 1891, AD 1045 and 1260, 2545, 2595, 3350, 3815, 4740, 7190, 9185 and 11 495 cal. yr BP. Dark-coloured SEs develop high-amplitude reflections in front of the deltas and in the deep central basin. These beds are mainly made of terrestrial organic matter (soils and ligno-cellulosic debris) and are interpreted as resulting from intense hyperpycnal flood event. Mapping and quantifying the amount of soil material accumulated in the Holocene hyperpycnal flood deposits of the sequence allow estimating that the equivalent soil thickness eroded over the catchment area reached up to 5 mm during the largest Holocene flood events. Such significant soil erosion is interpreted as resulting from the combination of heavy rainfall and snowmelt. The recurrence of flash flood events during the Holocene was, however, not high enough to affect pedogenesis processes and highlight several wet regional periods during the Holocene. The Holocene period is divided into four phases of environmental evolution. Over the first half of the Holocene, a progressive stabilization of the soils present through the catchment of Lake Ledro was associated with a progressive reforestation of the area and only interrupted during

the wet 8.2 event when the soil destabilization was particularly important. Lower soil erosion was recorded during the mid-Holocene climatic optimum (8000–4200 cal. yr BP) and associated with higher algal production. Between 4200 and 3100 cal. yr BP, both wetter climate and human activities within the drainage basin drastically increased soil erosion rates. Finally, from 3100 cal. yr BP to the present-day, data suggest increasing and changing human land use.

1   Introduction

Climate variability and seismicity represent serious natural concerns to modern societies in the Alps (e.g. Beniston et al., 2007). Actual climate models project that future climate warming in central Europe will bring more frequent extreme events and especially heavy precipitations and floods (Buma and Dehn, 1998; Christensen and Christensen, 2003; Beniston et al., 2007; Stewart et al., 2011). Flood hazards vary as a function of the hydroclimatic regime, position within the drainage basin and human interaction in the catchment (Wohl, 2000). Changes in the hydrological balance influence therefore the hydrological regime of the slopes and govern the type, rate and occurrence of natural extreme floods (Knox, 2000) and associated soil erosion (De Ploey et al., 1995; Cerdà, 1998; Raclot and Albergel, 2006) and can affect human activities and societies especially in mountainous environments (Dearing, 2006; Dearing et al., 2006).

The southern Alps in Italy are sensitive to natural hazards such as earthquakes and flash floods (Tropeano and Turconi, 2004; Barredo, 2007; Marchi et al., 2010; Lauterbach et al., 2012). Former studies suggested that precipitation regimes in this part of the Alps may have been affected by Atlantic influences at millennial and multi-centennial time scales (Magny et al., 2009, 2012). Over the last decade, different authors have also shown that lake sediments represent valuable archives to reconstruct past river discharges (Chapron et al., 2005; Bøe et al., 2006; Debret et al., 2010; Stewart et al., 2011; Wirth et al., 2011; Gilli et al., 2013) and past seismic events (Chapron et al., 1999; Schnellmann et al., 2002; Fanetti et al., 2008; Lauterbach et al., 2012).

In this paper, drainage basin descriptions of slope and soils are combined with seismic profiles and sedimentological analysis of lacustrine cores retrieved from peri-Alpine Lake Ledro, Italy. On the basis of the Holocene chronology and flood frequency reconstructions presented in Vannière et al. (2013) established on sediment cores, our results propose a new organic geochemistry approach to distinguish the sources of exceptional deposits attributed to natural hazards such as earthquakes or flash floods. This allows the reconstruction of past regional seismicity and wet regional periods during the Holocene.

2   Study area

The drainage basin of Lake Ledro covers 111 km^2, culminates at 2254 m a.s.l. and is today influenced by a subcontinental climate characterized by mean total annual precipitations of 900 mm, mean annual temperature of 8 °C and significant snowfalls in winter above 1500 m a.s.l. (Beug, 1964). Recent river corrections have been installed in the Massangla River (west of Lake Ledro) and the Pur River (south of Lake Ledro) in order to reduce the effects of flood events. Indeed, these two temporary torrential tributaries of Lake Ledro and their drainage network develop canyons or gullying on steep slopes, transport decimetric blocks and export the fine fraction to the lacustrine basin (Fig. 1). Lake Ledro (45°52′ N/10°45′ E) is a small basin (3.7 km^2, 2.6 km long, 1.3 km wide, 46 m deep) of glacial origin dammed by a frontal moraine along its eastern side at 653 m a.s.l., where the Ponale River forms the outlet of the lake draining into Lake Garda located 65 m a.s.l. Since AD 1929, the level of Lake Ledro has been regulated for hydroelectricity production between lakes Ledro and Garda.

The bedrock of the drainage basin of Lake Ledro is composed of Mesozoic rocks with Triassic dolomite and Jurassic and Cretaceous limestones. The steep slopes (> 30 %, 50 km^2, yellow areas in Fig. 1b) are formed by Quaternary glacial and fluvial deposits (Bollettinari et al., 2005) and are covered by forest and open landscape (> 2000 m a.s.l.). In contrast, two flat valleys (0–5 %, hatched red areas in Fig. 1b) correspond to the palaeolake Ledro maximal extension after glacier retreat and to the present-day alluvial plains of the Massangla and Pur rivers. These alluvial plains and the lake shorelines have been associated with agricultural areas and human settlements since at least the Bronze Age, corresponding at Lake Ledro to a period of development of lake-dwelling which declined around 3100 cal. yr BP (Magny et al., 2009). In addition, this part of the southern Alps was affected by five strong regional earthquakes over the last millennia (Guidoboni et al., 2007; Fig. 1a; Table 1).

3   Methods

The sedimentary infill of the lake was imaged in autumn 2007 by high-resolution seismic profiling (Fig. 2a). A 3.5 kHz pinger system navigated with a GPS was employed from an inflatable boat. A dense grid of profiles enabled us to establish the seismic stratigraphy of the lacustrine infill and allowed the determination of two coring sites: LL082 (14.6 m core length) in the central deepest basin (water depth: 46 m) and LL081 (9.9 m core length) in the eastern part of the central basin (water depth: 45 m) (Fig. 2c). These two cores were retrieved in areas lacking massive reworked material (Fig. 2), using the UWITEC piston corer from a platform. Continuous composite sections were defined using two parallel cores at each site. The stratigraphic correlation between the two

Table 1. Historical earthquakes documented by Guidoboni et al. (2007) close to Lake Ledro (http://storing.ingv.it/cfti4med/).

Year	Location	Distance from Lake Ledro	Equivalent magnitude M_e	Epicentral intensity at epicentre I_0
AD2004	Salo	∼ 35 km SSW		VIII
AD 1901	Salo	∼ 35 km SSW	5.7	VIII
AD 1891	Illasi valley	∼ 55 km SE	5.9	VIII-IX
AD 1117	Verona	∼ 53 km SSE	6.8	IX
AD 1046	Adige valley	∼ 25 km E	6	IX

coring sites is supported by the identification of characteristic lithological layers and the seismic stratigraphy. Initial core analysis of LL082 and LL081 included gamma-ray attenuation density measured with a GEOTEK multi-sensor core logger (sampling interval: 0.5 cm), macroscopic core description and digital photographs. Punctual laser diffraction grain-size measurements were performed using a Malvern Mastersizer 2000 on several sedimentary event (SE) samples. Age–depth models of lacustrine cores are based on gamma-spectroscopic radionuclide measurements (^{137}Cs, ^{210}Pb) on core LL082 and 19 AMS radiocarbon dates (6 on LL082 and 13 on LL081, Fig. 3a) that are reported in Table 2 and discussed in Vannière et al. (2013).

In July 2011, 11 complete pedological profiles and 6 (dry) river beds were sampled within the watershed (coloured circles in Fig. 1b). They were selected at different altitudes and under various vegetation covers in order to be representative of (i) high-altitude thin soils composed of lithic and rendzic Leptosols (62 % of the catchment area), (ii) well-developed soils composed of Cambisols (21 % of the catchment area) and (iii) alluvial soils divided into colluvic Regosols and Fluvisols (17 % of the catchment area).

Organic geochemistry of lake sediments and catchment area samples was measured by Rock-Eval pyrolysis (RE) and quantitative organic petrography (QOP). RE is used to characterize the organic content of natural samples by thermal cracking (Espitalié et al., 1985; Behar et al., 2001). RE parameters such as the total organic carbon (TOC, %), the S2 (i.e. the amount of hydrocarbon that escapes from the sample during the thermal cracking, expressed in mgHC) and the thermal maturity (Tpeak, °C) measurements can be used to characterize soil organic matter (Di Giovanni et al., 1998; Sebag et al., 2005; Copard et al., 2006) and to discriminate between an aquatic or terrestrial origin of the organic matter into lacustrine environments (Talbot and Livingstone, 1989; Simonneau et al., 2013). S2 represents the total amount of hydrocarbon that escapes from the sample during the thermal cracking (Ariztegui et al., 2001). The regression lines (slopes) of the diagram S2 vs. TOC determine constant values of the hydrogen index (HI, expressed in mgHC g^{-1}TOC) since HI = (S2 · 100)/TOC (Behar et al., 2001). In this diagram, the matrix effect, essentially due to clay particles which can retain the hydrocarbon
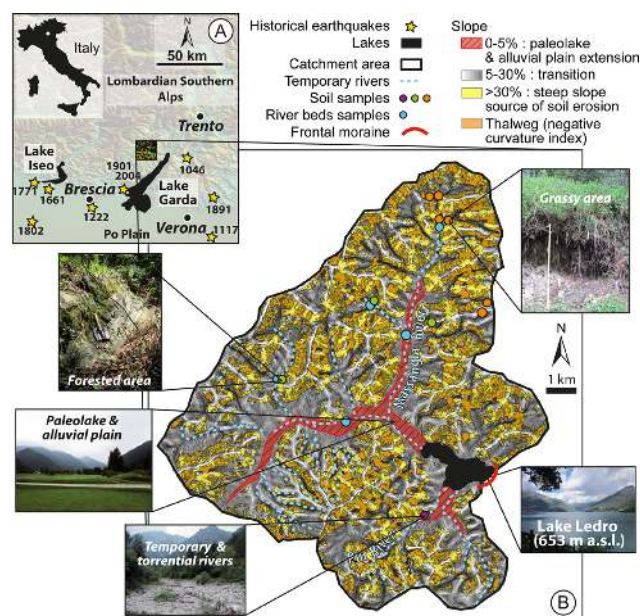

Fig. 1. Location of Lake Ledro in the Italian Alps (**A**) and geomorphological characteristics of its catchment area (**B**). The Trento area is an active seismic region highlighted by historical earthquakes (yellow stars). Catchment area of Lake Ledro is mainly defined by temporary rivers and steep slopes where soil and river samples have been collected.

produced from the cracking of the organic matter (Ariztegui et al., 2001), can be shown by the positive x intercept of the regression lines with the TOC axis. Classically, two particular slopes, corresponding to HI equal to 750 and 300 mgHC g^{-1}TOC, respectively, are represented in the S2 vs. TOC diagrams in order to identify the chemical quality or the origin of the organic compounds (Ariztegui et al., 2001). Values of HI inferior to 300 mgHC g^{-1}TOC can point towards organic matter oxidation in the sediment or a contribution of terrestrial material (Ramanampisoa and Disnar, 1994; Disnar et al., 2003; Calvert, 2004; Jacob et al., 2004; Simonneau et al., 2013). Inversely, HI values superior to 300 mgHC g^{-1}TOC suggest well-preserved organic matter in the sediment or higher contributions of lacustrine algal particles, the specific pole of which is represented by HI values superior to 750 mgHC g^{-1}TOC (Talbot and Livingstone, 1989). The Tpeak reflects the maximal temperature reached during the S2.

QOP developed by Graz et al. (2010) is based on the optical identification and quantification of the organic fraction after elimination of carbonate and silicate phases by hydrochloric and hydrofluoric attacks. Components are characterized by their optical properties (colour and reflectance), their forms (amorphous or figurative) and their origins (algal, phytoclastic or fossil) (Combaz, 1964; Tyson, 1995; Di Giovanni et al., 2000; Sebag et al., 2006; Simonneau et al., 2013). Excluding the standard, which was deliberately added into preparations, three main types of organic particles have
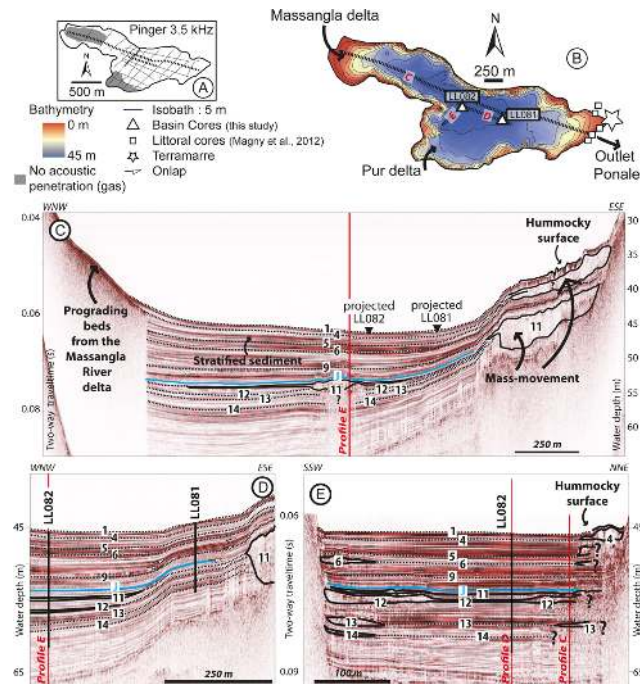
Fig. 2. Seismic stratigraphy of Lake Ledro, based on a dense grid of profiles (**A**). The bathymetric map is generated from the seismic data (**B**). Three main profiles, C, D and E, are selected to show the different acoustic facies. Numbers 1 to 14 correspond to some light-coloured sedimentary events identified in cores.

Fig. 3. Core-to-core correlation between LL081 and LL082 (**a**) and selected digital photographs of core sections (**b**) illustrating the occurrence of sedimentary events intercalated within the background sedimentation. The chemical composition of both the background sedimentation and the sedimentary events is also illustrated. Black stars show the depths of available dates given in Table 2 and black triangles locate samples analysed by organic geochemistry in this study.

been used in this study: red or grey amorphous particles (rAP and gAP, respectively) and lignocellulosic fragments (LCF), whose significations are given from analysis results (see Sect. 4.3 below).

4   Results

4.1   Seismic basin analysis

The bathymetric map of Lake Ledro (Fig. 2b) was calculated by interpolating the seismic data (Fig. 2a) and highlights the occurrence of steep slopes surrounding a relatively wide and flat central basin. The morphology of the glacial or bedrock substrate is seismically imaged in many areas and suggests that the sediment infill reaches a thickness of more than 40 m in the central basin (Fig. 2c). Downlapping geometries just basinward from the western and southern areas lacking seismic penetration indicate prograding beds from the Massangla and Pur river deltas, respectively (Fig. 2c). In the deepest part of the basin, sediments are thickest, well stratified and characterized by high-amplitude reflections, which have a spacing that becomes thinner towards the eastern edge of the basin (Fig. 2c). Some reflections (such as J, Fig. 2) delimited by deltas and bedrock on the northern coast are defined by forming the top of transparent thin units whose extensions
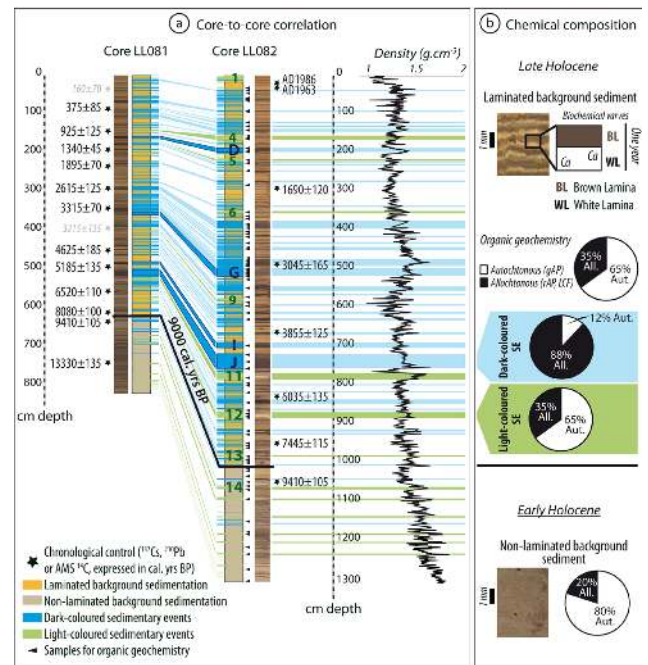
are limited by onlap configurations toward the eastern edge of the central basin (Fig. 2d).

Many transparent-to-chaotic lens-shaped bodies of various sizes are also present and coeval within the lacustrine basin. Events 4 and 11 (Fig. 2) are for instance described by nine and ten coeval independent bodies, which are interpreted to be the result of mass-wasting processes along the subaquatic slopes (e.g. Schnellmann et al., 2002). The thicker lens-shaped bodies (event 11) turn into a thin layer bearing few discontinuous reflections in the deepest part of the lake. The reflections connecting the tops of all coeval mass-wasting deposits are picked as seismic-stratigraphic horizons for each event (Fig. 2). They represent isochrones and coincide with the thickest SEs recognized in LL082 and LL081 (SE 1, 4, 5, 6, 9, 11, 12, 13 and 14, Table 3, Figs. 2 and 3a). The event horizon can be traced throughout the lake basin, except in windows of no acoustic penetration. They also allow seismic-to-core correlations between the two coring sites (Fig. 2d).

Table 2. Radiocarbon dates obtained from Lake Ledro sediment sequences LL082 and LL081. Age calibration was done using the program Calib 6.06 (Reimer et al., 2009). The two dates in italic (POZ-27888 and POZ-30222) have been rejected (see Vannière et al., 2013, for more details).

Method	Material	Laboratory	MC depths (cm)	Radiocarbon ages	Calibrated ages (cal. yr BP)
		Core LL082			
AMS ^{14}C	Leaf remains	ETH-39232	303	1765 ± 35	1690 ± 120
		ETH-40410	493.5	2890 ± 50	3045 ± 165
		ETH-10411	666	3575 ± 35	3855 ± 125
	Leaf remains and needles	ETH-39233	840	5200 ± 35	6035 ± 135
	Needles	ETH-39234	960.5	6530 ± 40	7445 ± 115
		ETH-39235	1065.5	8405 ± 40	9410 ± 105
		Core LL081			
AMS ^{14}C	Wood Peat Charcoal	*POZ-27888*	*16.5*	255 ± 30	160 ± 70
		POZ-30216	82	290 ± 30	375 ± 85
		POZ-30218	142	1020 ± 30	925 ± 125
		POZ-30219	194	1445 ± 30	1340 ± 45
		POZ-30220	239	1945 ± 30	1895 ± 70
		POZ-30221	299	2520 ± 35	2615 ± 125
		POZ-27890	351	3095 ± 30	3315 ± 70
		POZ-30222	*402.5*	3030 ± 35	3215 ± 135
		POZ-27891	461.5	4080 ± 35	4625 ± 185
		POZ-30223	499	4550 ± 35	5185 ± 135
		POZ-27892	562.5	5720 ± 40	6520 ± 110
		POZ-30224	616	7270 ± 50	8080 ± 100
		POZ-27894	641.5	8385 ± 35	9410 ± 105
		POZ-27895	759.3	$11\,480 \pm 60$	$13\,330 \pm 135$

4.2 Physical properties of lacustrine sediment and sedimentary events

Cores LL081 and LL082 are mainly composed of Holocene sedimentary sequences reaching 6.9 m and 11.70 m length, respectively (Fig. 3a). Before 9000 cal. yr BP and back to 13 330 cal. yr BP (i.e. below 620 and 1020 cm core depth) in cores LL081 and LL082, respectively, the background sediment is not laminated and is only interrupted by few SEs. After 9000 cal. yr BP, the succession becomes finely laminated in the background sediment. Based on thin sections on a selected part of core LL082, core scanner XRF analysis and high-resolution digital photographs (Wirth et al., 2012; Vannière et al., 2013), laminated background sedimentation is made of a succession of millimetric to inframillimetric couplets of discrete white calcite layers (WL, Fig. 3b) and brown organic layers (BL, Fig. 3b) typical of calcite varves (Lotter and Lemcke, 1999; Brauer et al., 2008; Czymzik et al., 2010) reflecting the succession of summer (WL) and winter (BL) seasons. Grey clayey iron-rich layers are, in addition, frequently occurring at different positions within the varved sequence (Wirth et al., 2012) and are interpreted as thin detrital layers (i.e. small-scale flood

deposit, cf. Czymzik et al., 2010). During the Holocene laminated background sedimentation, the occurrence of SEs increases (Fig. 3a) in both cores, interrupting the annual succession. SEs are characterized by specific colour, bulk density and grain-size (Figs. 3a and 4), clearly contrasting with the background sedimentation. SEs represent a cumulative length of almost 5 and 2.5 m length of the Holocene sequence in LL082 and LL081, respectively. Two kinds of SEs are easily identified from the Holocene background sediment based on their thickness (centimetric to pluricentimetric layers), colour (dark or light), texture (graded or massive) and density data. As discussed in Vannière et al. (2013), the identification of these two types of SEs at both coring sites highlights a good core-to-core correlation between LL081 and LL082 and suggests that these SEs usually affect a major part of the deep basin since only a few layers are documented in LL082, as for example the light-coloured deposit 1 (Fig. 3a). Because all these SEs are generally characterized by higher densities than the background sediment, their frequent occurrence in the basin fill can explain the relatively high-amplitude reflections identified with a high frequency in seismic data in the entire deep basin. For analytical reasons, only SEs thicker than 1 cm could be sampled, and are considered in the
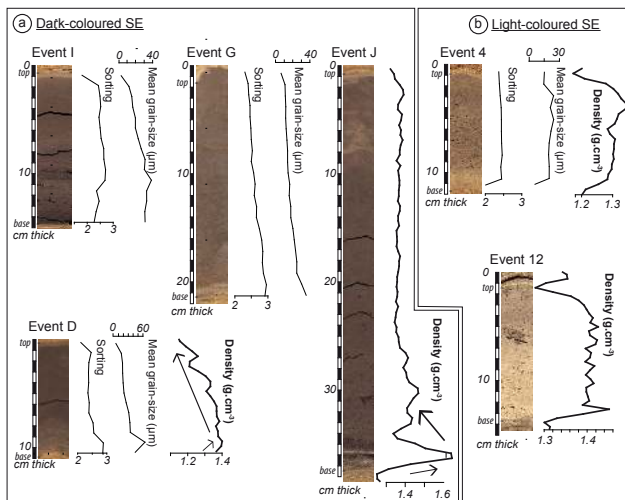
Fig. 4. Grain-size parameters and sediment bulk density profiles are given in **(a)** for selected dark-coloured sedimentary events (events D, G, I and J) and in **(b)** for selected light-coloured sedimentary events (events 4 and 12).

following sections. It means that we are here not discussing thin events (below 1 cm) and flood frequency, which are included in the study of Vannière et al. (2013).

Dark-coloured SEs (labelled by letters) are graded beds and are characterized by a sharp increase of density at their base, progressively decreasing towards the top (Figs. 3b and 4a). Some organic debris were identified within these dark-coloured SEs and sampled for radiocarbon dating (cf. Vannière et al., 2013). Mean grain-size in most of these dark-coloured SEs highlights the development of inverse (coarsening upward) and normal (fining upward) grading (from 44 to 64 and then 4 µm and from 31 to 39 and then 2 µm in events D and I, respectively; Fig. 4a). Some dark-coloured SEs are, however, only characterized by normal grading (e.g. from 35 to 6 µm in event G, Fig. 4a). In addition, all dark-coloured SEs are not well sorted (sorting values > 2), but sorting is always increasing at the top of the deposits and associated with the formation of a thin clay cap (Fig. 4a). Dark-coloured SEs thicker than 1 cm are relatively frequent (73 events during the Holocene), have a wide range of thicknesses (from 1 to 38 cm) and have mean grain-size < 30 µm (Fig. 4a) on average.

Light-coloured SEs (labelled by numbers) thicker than 1.5 cm are comparatively less frequent (13 events during the Holocene), less variable in thicknesses (ranging from 1.5 to 13 cm) and slightly thicker on average (5.25 cm). They are in addition much more massive both in terms of mean grain-size and density (Figs. 3a and 4b). These light-coloured SEs are also made of smaller particles (mean grain-size < 25 µm; Fig. 4b).

4.3 Soil and lacustrine sediments organic characterization

Soils in the drainage basin vary strongly according to elevation. High-altitude thin soils are present above 1100 m a.s.l. They are not very developed as they show no accumulation or eluviation layers, are rich in calcareous gravels and do not exceed 30 cm in thickness. They form on the calcareous bedrock and are composed of two main silty or sandy layers associated with various amounts of calcareous gravels ranging from 0 to 15 %. Well-developed soils are found between 800 and 1100 m a.s.l. They are located in forested areas, do not exceed 70 cm in thickness and form over fissured limestone bearing up to 80 % gravels. Finally, alluvial soils are found in the alluvial plain of the flat valleys. They are characterized by a silty texture and can reach 80 cm in thickness.

The S2 vs. TOC diagram of soil and riverbed samples show that for various TOC content (ranging from 0.09 to 29.4 %) all samples are systematically near or below the line representing HI (see Sect. 3) equal to 300 mgHC g^{-1}TOC (Fig. 5a). In agreement with Sebag et al. (2005), S2 curves from soil samples can be linked to the vegetation cover: in superficial layers from grassland soils within the drainage basin of Lake Ledro, the chart S2 vs. temperature shows a unimodal symmetric curve with Tpeak around 462 °C, whereas in superficial layers from forested soils the chart shows a bimodal dissymmetric curve with Tpeaks around 378 and 455 °C (Fig. 5b).

QOP highlights that watershed samples are composed of two major groups of organic particles: (1) non-pollen microfossil particles, consisting of colloidal red amorphous particles defined by diffuse external limits and without internal structures (rAP, Fig. 5c), cuticles and lignocellulosic fragments (LCF, Fig. 5c) and opaque particles without high reflectance; and (2) pollen microfossil particles composed of spores and pollens. The rAP and the LCF identified in this study are similar to those described by Di Giovanni et al. (1998), Graz et al. (2010) or Simonneau et al. (2013) and associated with soil particles (rAP) and upper vegetation debris (LCF) coming both from the watershed. Variations in the values of the rAP/LCF ratio can be used to disentangle the impact of land use and climate during the Holocene on the vegetal cover, soil erosion and sediment load of rivers in Alpine environments (cf. Noël et al., 2001; Arnaud et al., 2005; Dearing, 2006; Dearing et al., 2006; Jacob et al., 2009; Simonneau et al., 2013).

Holocene lacustrine samples from core LL082 (Fig. 3a) were taken from the SEs and the background sediment. SEs (Fig. 6a) are always defined by HI values lower than 300 mgHC g^{-1}TOC and thus systematically lower than background sediment samples (for the same TOC) whose HI values are higher than 300 mgHC g^{-1}TOC (Fig. 6a). Regression lines are calculated for background sediment and SE samples and show that light-coloured SEs are not identified by a specific domain but are located between the

Table 3. Estimated ages and characteristics of SEs interpreted as subaquatic mass-movements triggered in Lake Ledro by regional earthquakes as discussed in the text.

| Events	Thickness in core LL082 (cm)	Estimated ages inferred from Vannière et al. (2013)	Regional earthquakes	Numbers of associated mass wasting deposits	Likelihood of earthquake triggering
SE 1	11.8	AD 2005 ± 3	Salo (AD 2004)	2	Very high
SE 2	1.5	AD 1871 ± 39	Salo (AD 1901)	?	High
SE 3	1.5	AD 1863 ± 42	Illasi valley (AD 1891)	?	High
SE 4	10.8	AD 1044 ± 127	Verona (AD 1117) or Adige valley (AD 1046)	9	Very high
SE 5	4.4	1256 ± 115 cal. yr BP		3	High
SE 6	5.3	2545 ± 104 cal. yr BP	Iseo event (2525 ± 110 cal BP)	5	Very high
SE 7	1.6	2595 ± 102 cal. yr BP		?	High
SE 8	2.9	3348 ± 79 cal. yr BP		?	Moderate
SE 9	4.6	3815 ± 84 cal. yr BP		2	High
SE 10	1.5	4742 ± 156 cal. yr BP	Iseo event (4488 ± 110 cal BP)	?	High
SE 11	16.1	5889 ± 92 cal. yr BP		10	High
SE 12	13	7190 ± 127 cal. yr BP		10	High
SE 13	5	9183 ± 84 cal. yr BP		2	High
SE 14	4.6	11 493 ± 339 cal. yr BP		2	High
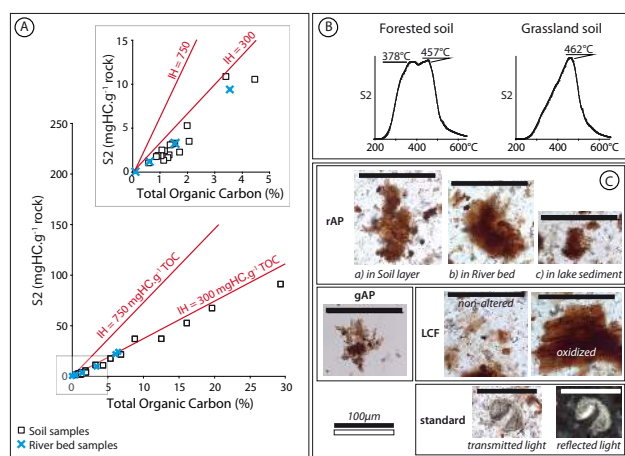
Fig. 5. Rock-Eval results **(A)** of soil and riverbed samples are represented by the diagram S2 vs. (%). The two linear domains of the hydrogen index (HI = 750 and HI = 300 mgHC g^{-1} TOC) corresponding to algal and terrestrial poles, respectively, are represented. S2 curve **(B)** from Rock Eval analysis on superficial layers from forested and grassland soils are also presented. Thermal cracking of the hydrocarbon compounds are represented by the temperature. Organic particles identified by quantitative organic petrography are illustrated in **(C)**: rAP in soil layers, riverbeds and lacustrine sediment; gAP; LCF non-altered or oxidized; and the standard added in transmitted and reflected light modes.

two others. The matrix effect is equal for background sediment and dark-coloured SE samples, representing 0.3 % of TOC. QOP performed on the same set of lacustrine samples only differs from the watershed samples by the presence of grey amorphous particles (gAP, Fig. 5c). However, the proportion of rAP, gAP and LCF is different between background sediment and SE since background sediment samples and light-coloured SEs are mainly composed of gAP (in mean, gAP = 65 %, rAP = 13 % and LCF = 22 %), whereas dark-coloured SEs are essentially composed of rAP (in mean, rAP = 59 %, gAP = 12 % and LCF = 29 %, Fig. 6b). Only two dark-coloured SE samples are dominated by gAP and correspond to samples rich in clays at the top of the deposit (clay cap; Figs. 4a and 6b, red squares).

5 Discussion

5.1 Origins of sedimentary events

As shown in Figs. 5 and 6, the organic fraction of background sediments in Lake Ledro is composed of LCF, rAP and gAP, while soil and riverbed samples are only composed of rAP and LCF. The gAP are only found in background lacustrine sediment samples and typically result from lacustrine algal productivity (Sifeddine et al., 1996; Di Giovanni et al., 1998).

This optical organic identification is also in agreement with RE results since (i) all HI values below 300 mgHC g^{-1} TOC are measured in soil and riverbed samples and characteristic of a terrestrial pole (Simonneau et al., 2013) and (ii) intermediate HI values of background lacustrine sediment samples lie between the algal pole (750 mgHC g^{-1} TOC; Talbot and Livingstone, 1989) and the terrestrial one (300 mgHC g^{-1} TOC).
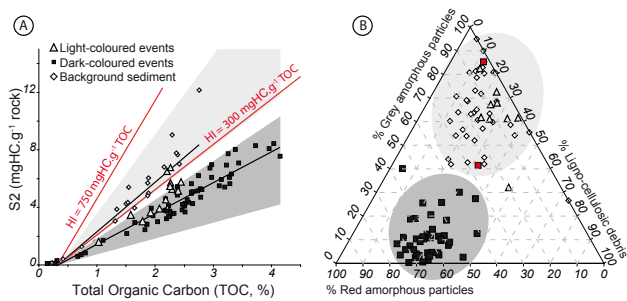
Fig. 6. Organic geochemistry of core LL082. Rock-Eval results **(A)** are represented by the diagram S2 vs. TOC (%). White triangles and black squares represent samples taken in light-coloured events or in dark-coloured ones, respectively. Samples taken within the background sedimentation are represented by white diamonds. Solid lines indicate the regression line for background sediment samples and dark-coloured events samples, respectively. Specific organic signature is given by quantitative organic petrography **(B)** represented on a triangular diagram showing the mass percentage of grey amorphous particles, red ones and lignocellulosic debris making up each sample. In this diagram, the red squares represent samples taken in the clay caps, which cover the top of two dark-coloured events.

5.1.1 Light-coloured SEs and earthquakes

Light-coloured SEs are mainly composed of gAP similar to the ones observed throughout the background sediment and previously identified as resulting from algal growth in the lake waters. This therefore suggests a common origin between the two sedimentary facies. Besides, HI values ($< 300\,\mathrm{mgHC\,g^{-1}TOC}$) do not correspond here with higher terrestrial inputs but specify that the organic matter in these light-coloured SEs is more degraded than in the background sediments. This oxidation suggests that light-coloured SEs consist of redeposited background lacustrine sediment that became mobilized and oxidized in the water column. This interpretation is in agreement with the seismic data indicating that these light-coloured SEs are restricted to the central basin of the lake. Moreover, some light-coloured SEs are contemporaneous to several subaquatic mass-wasting events affecting the steep slopes of the lake (Figs. 2, 7d and e). The constant mean grain-size and the stable values of sorting in these light-coloured SEs (Fig. 4b) are in addition typical of mass-flow deposits (Mulder and Cochonat, 1996). The latter are therefore interpreted as distal mass-flow deposits. Event 1, only identified in core LL082 (Fig. 3a), is composed of tilted finely laminated sediments. This event 1 is too thin (12 cm thick) to be clearly identified in seismic data, but it appears contemporaneous to hummocky morphologies identified on the eastern and northern parts of the basin (Fig. 2).

As discussed in Vannière et al. (2013), radionuclide measurements in core LL082 revealed that event 1 consists of a superposition of two equal recent sedimentary sequences. Altogether these characteristics of event 1 are typical from
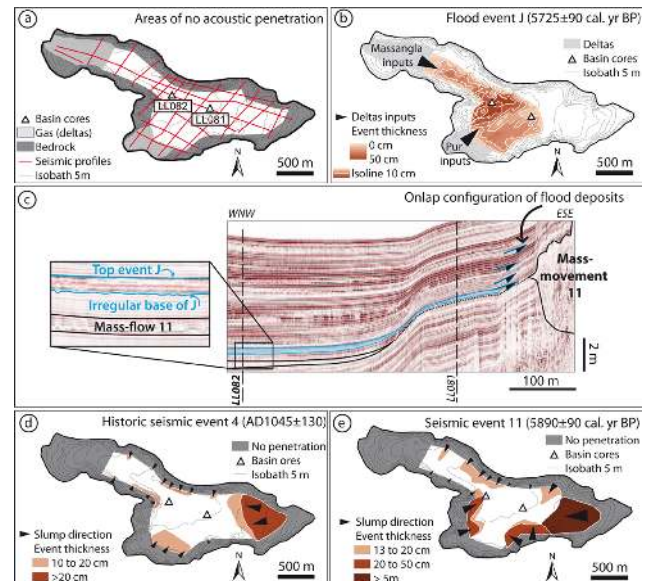

Fig. 7. Grid of the 3.5 kHz seismic survey acquired for this study in Lake Ledro and windows of no acoustic penetrations (due to coarse and gas-rich deltaic sediments or bedrock occurrence) are localized **(a)**. **(b)** illustrates the distribution and thickness of hyperpycnal flood event J characterized by an erosive base and the development of onlap configurations on seismic profiles **(c)**. In **(d)** and **(e)** the distribution and thickness of mass-flow deposits caused by historical earthquake event 4 and by prehistorical event 11 **(e)** are illustrated and clearly contrasting with the ones of flood event J.

the initial stage of a thin slide deposit in the central basin favoured by a limited displacement of recent sediments along several slopes of the lake basin (i.e. creeping phenomena developing hummocky morphologies). This event 1 is dated to AD 2005 ± 3 and therefore consistent with the Salo earthquake in AD 2004, the epicentre of which being located at only 35 km SW from Lake Ledro (Fig. 1, Tables 1 and 3). This earthquake could therefore be the trigger event for the development of creeping along the slopes and the formation the slide event 1 in the central basin.

The next two older mass-flow deposits, reaching at least 1.5 cm in thickness in the sediment cores (Fig. 8a, events 2 and 3), are dated to AD 1870 ± 40 and AD 1860 ± 40 and are synchronous, within the dating error of the sediment core, with two historic earthquakes from AD 1901 and AD 1891, respectively (Fig. 1, Tables 1 and 3). Light-coloured SE 4 (Fig. 4b) is dated to 905 ± 130 cal. yr BP (AD 1045 ± 130) and associated with numerous coeval mass-movements along the basin slopes (Fig. 7d, Table 3), which are the typical signature of large earthquakes in lakes (Schnellmann et al., 2002; Lauterbach et al., 2012). Lake Ledro is located only 50 km NE from Verona (Fig. 1a), where a catastrophic seismic event occurred in AD 1117 (Table 1; Guidoboni and Comastri, 2005), and it is near the Adige valley affected by an earthquake in AD 1046 (Fig. 1a; Table 1; Guidoboni et al.,
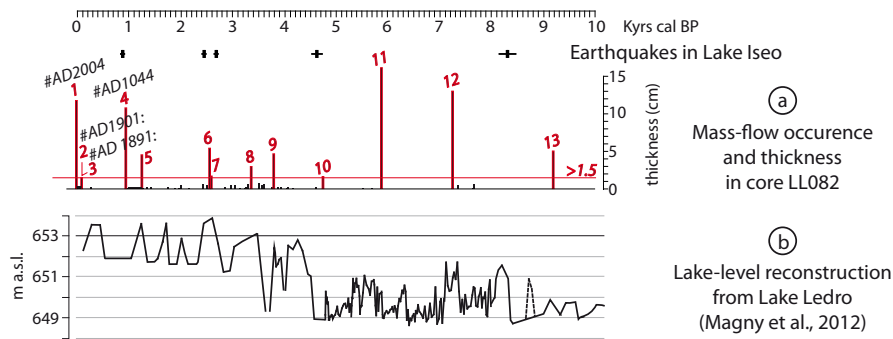
Fig. 8. Illustration of mass-flow occurrence, thickness and age in core LL082 **(a)**. Some mass- flow deposits superior to 1.5 cm thick are contemporaneous to historical earthquakes (#) and prehistorical earthquakes (+) documented in nearby Lake Iseo by Lauterbach et al. (2012). Holocene lake level evolution from Lake Ledro **(b)** reconstructed by Magny et al. (2012).

2007). Event 4 could therefore be likely the consequence of one of these two regional historical earthquakes. In core LL082, pre-historical mass-flow deposits thicker than 1.5 cm are dated to 1255 ± 115, 2545 ± 105, 2595 ± 100, 3350 ± 80, 3815 ± 85, 4740 ± 155, 7190 ± 130, 9185 ± 85 and $11\,495 \pm 340$ cal. yr BP (Table 3, Fig. 8a). Some of them are, within the age–depth model errors, synchronous with pre-historical earthquakes recorded in nearby Lake Iseo (2430 ± 105, 2545 ± 105, 2595 ± 100 and 4745 ± 155 cal. yr BP; Figs. 1a and 8a; Lauterbach et al., 2012) and suggest that they were triggered by large regional earthquakes (Table 3). The others light-coloured mass-flow deposits in Lake Ledro are supposed to correspond to previously undocumented local earthquakes around 3350 ± 80, 3815 ± 85, 7190 ± 130, 9185 ± 85 and $11\,495 \pm 340$ cal. yr BP (Table 3). Event 11, dated between 5800 and 5980 cal. yr BP, has probably a seismic origin since this event is associated with the largest coeval mass-movements (Figs. 2c and 7e) that occurred in Lake Ledro during the Holocene (Table 3). Among the 14 seismic events recorded in Lake Ledro during the Holocene (Fig. 8a, Table 3), ten events occurred during the last 5000 yr, i.e. during a period characterized by higher lake levels, based on a series of littoral cores (Magny et al., 2012) (Figs. 2b and 8b). These higher levels may have therefore favoured slope instabilities and increased the sensitivity of Lake Ledro to regional seismo-tectonic activity. Otherwise, this could also result from a higher seismicity over the last 5000 yr.

5.1.2 Dark-coloured SEs and flood deposits

Dark-coloured SEs in Lake Ledro present the same organic signature as those of the watershed samples since they are essentially composed of terrestrial components similar to the ones identified throughout the drainage basin (rAP and LCF, Fig. 5b) and characterized by HI values clearly below 300 mgHC g^{-1} TOC. In addition, laser grain-size and bulk density measurements in these beds clearly indicate that most of their bases are successively inversely and normally graded. This is the typical signature of hyperpycnal flood deposits in a subaquatic basin (Mulder and Alexander, 2001;

Mulder et al., 2003; Mulder and Chapron, 2011; St-Onge et al., 2012), where the coarsening upward and the fining upward sequences are correlated to the rising and the falling limb of a flood hydrograph, respectively. The very thin basal unit of event J (Fig. 4a), compared to the thick upper unit, implies therefore an asymmetric flood hydrograph, which is typical of hyperpycnites and corresponds to the succession of the waxing and waning flows (St-Onge et al., 2004; Mulder and Chapron, 2011). Because the preservation of the waxing unit of a hyperpycnite at a given location in a basin is typically linked to (i) the flood hydrograph, (ii) the peak intensity of the flood event and (iii) the proximity of the tributary (Mulder et al., 2003), dark-coloured SEs characterized only by a fining upward sequence (such as event G) at coring sites LL081 and/or LL082 in Lake Ledro can be related to exceptional flood events whose peak intensities were high enough to erode the waxing unit. In addition, the significant occurrence of algal particles in the clay caps of dark-coloured SEs is interpreted as resulting from the remobilization in the water column of lacustrine sediments at the lake floor during the development of the hyperpycnal current (Chapron et al., 2007). These clay caps would therefore essentially result from the settling of fine-grained particles suspended near the lake floor at the end of the flood event.

Dark-coloured SEs in Lake Ledro are thus interpreted as hyperpycnal flood deposits largely composed of soil material and vegetation debris eroded from the drainage basin and brought in the lake by heavy precipitation and/or snowmelt events. Because Massangla and Pur rivers are temporary torrential tributaries draining steep slopes, dark-coloured SEs in Lake Ledro likely reflect flash flood events (Lambert and Giovanoli, 1988; Bornhold et al., 1994; Gilli et al., 2013). The large flood deposit marked by dark-coloured SE J is thick enough to be mapped along seismic profiles (Fig. 7c). It reaches up to 6.4×10^5 m^2 of area, extends from the Massangla and Pur delta slopes towards the central basin where it forms an up to 50 cm-thick depocenter (Fig. 7b) and develops onlaping geometries at the eastern edge of the central basin (Fig. 7c).

5.2 Flood events and soil erosion

Since flood deposits in Lake Ledro are essentially composed of soil-derived material, it is necessary to estimate the amount of pedological material eroded during exceptional flood events from the catchment area, in order to test if their occurrence in the lake basin can be used as a good proxy to reconstruct the palaeohydrology of the study area.

The spatial extensions of the hyperpycnal floods recorded into Lake Ledro are given by their eastern onlap configurations of their high-amplitude reflections in the central basin (Figs. 2d and 7c). Densities of soil surface layers sampled in the catchment area vary from 1.04 to 1.7 g cm^{-3} (on average 1.3 g cm^{-3}) and are close to ones measured in flood deposits from sediment cores (on average 1.4 g cm^{-3}). The calculated volume of terrestrial fine fraction eroded during a flash flood is thus assumed as representative of the total terrestrial material eroded within the erodible surface of the catchment area. It is calculated by multiplying the mean thickness of a specific dark-event deposit by the mean spatial extent of Lake Ledro hyperpycnal flood events (evaluated to 3.3×10^5 m^2 on average, Fig. 7b) and by the percentage of terrestrial material inside (determined by QOP). Such an approach only slightly underestimates (by 7 %) the accurate volume of event J which could be precisely mapped on seismic sections (Fig. 7b).

For each flood event, this volume represents mechanical erosion of an unknown thickness of soil within a certain percentage of the erodible surface source of terrestrial material. De Ploey (1991), Cerdà (1998, 1999), Le Bissonnais et al. (2001), Souchère et al. (2003) and Girard et al. (2011) described the cumulative effects of gullying on the thalwegs and on slopes steeper than 30 % as the two main factors controlling soil erosion within a drainage basin under a given vegetation cover. Analysing the digital elevation model, we consider that the topography was constant during the entire Holocene period and intersect the two key criterions (thalwegs and slopes > 30 %, Fig. 1b, orange and yellow areas, respectively) in order to map source areas of terrestrial material (~ 23.3 km^2 in the catchment). Flat alluvial valley slopes (0–5 %, Fig. 1b, hatched red areas, 0.8 km^2 in the catchment) are mainly sites of accumulation processes; however, the material stored in these valleys can be remobilized during flood events (Girard et al., 2011). We consider therefore that slopes between 0 and 5 % can also be affected by erosion processes during a flash flood event. The equivalent thickness of soil eroded corresponding to 100 % of these source areas affected by erosion represents the minimum equivalent soil thickness which can be eroded by a given flood event. It is more difficult to determine this value for thinner flood events, which represent low terrestrial volumes (black curve, flood event of 2 cm thick in LL082, Fig. 9), than for thicker events (grey curve, flood event J, 38 cm thick in LL082, Fig. 9). The prehistorical major hyperpycnal flood event F (18 cm thick into core LL082, Fig. 10b) is the example presented in Fig. 9. It
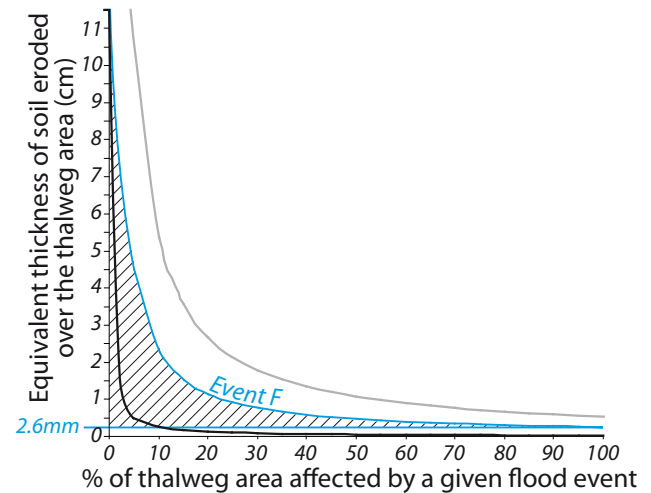

Fig. 9. Illustration of the steps used to estimate the equivalent soil thickness eroded over the catchment area associated with a flood deposit in Lake Ledro.

is on average composed of 90 % allochtonous components, which correspond to 53 460 m^3 of accumulated terrestrial material. Considering this volume, at least 2.6 mm of equivalent soil thickness, within the catchment area of Lake Ledro, were eroded by this flash flood event (blue curve, Fig. 9). Similarly, we can estimate that events G and J (Fig. 10b) eroded at least 3 mm and 4.9 mm of equivalent soil thickness in the watershed of Lake Ledro, respectively.

This approach highlights that extreme events eroded at least a few millimetres of soil over the watershed and correspond to values described by Raclot and Albergel (2006) for areas affected by modern water erosion and runoff. Their recurrence in time can be problematic and can affect the pedogenesis process at long time scales, since Duchaufour (1983) stated that well-developed soil pedogenesis such as that described in the Lake Ledro catchment area is relatively slow. However, events F, G and J are exceptional in intensity since they are the only ones to reach such thicknesses during the Holocene. This indicates that the pedogenesis in the Lake Ledro watershed is not significantly affected by the recurrence of flash flood events and suggests that the Lake Ledro flood sequence offers a reliable record to track the evolution of precipitation regimes during the Holocene in this part of the Alps.

5.3 Climatic significance of flash flood deposits in Lake Ledro

It is well known that rainfall events have to reach a certain threshold in magnitude, duration, intensity or discharge to trigger erosional processes and flooding in drainage basins (De Ploey et al., 1995; Mudelsee et al., 2003; Marchi et al., 2010). According to Mulder et al. (2003) there is also a positive relationship between the flood deposit thickness,

the river discharge and the rain intensity. Several recent studies focusing on modelling of snowmelt erosion have, however, shown that this process could export a large amount of soil particles (60 %) especially on grasslands where the snowmelt runoff coefficient is higher (Ollesch et al., 2006; Tanasienko et al., 2009 and 2011). Consequently, we suggest that Holocene flash flood deposits in Lake Ledro result from the combination of heavy rainfalls and snowmelt phenomena.

5.4 Climate and human interactions on terrestrial and lacustrine Holocene environment at Lake Ledro

The most important parameters discussed below are depicted in Fig. 10, where the hyperpycnal flood occurrences and thicknesses documented by Lauterbach et al. (2012) in nearby Lake Iseo (Figs. 1a and 10a) are compared to the hyperpycnal flood occurrences and thicknesses identified in Lake Ledro (Fig. 10b). This comparison suggests the occurrence of wetter periods favouring flooding activity at a regional scale in the Italian southern Alps (Fig. 10). During the first half of the Holocene, the mean flood intervals from lakes Iseo and Ledro are equalled to 4.8 and 4 events by millennia, respectively, whereas after around 5000 cal. yr BP they increased to 8.4 and 9.2 events by millenia, respectively. These changes in flood return times suggest that (i) the two lakes are sensitive to the same climatic influences and that (ii) the second half of the Holocene was wetter, which is in agreement with the higher lake levels documented by Magny et al. (2009, 2012) at Lake Ledro. Over the last 500 yr, the last wetter period recorded by hyperpycnal flood deposits in the southern Alps (Fig. 10b) occurred between ca. AD 1600 and AD 1850 and matches the second phase of the well-documented Little Ice Age period (Chapron et al., 2002; Wanner et al., 2011; Magny et al., 2010).

Furthermore, the ratio rAP/LCF (see Sect. 4.3), the S2 curves from Rock-Eval pyrolysis and the HI are compared and discussed between the results obtained from samples taken in the background sedimentation or in flood events (Fig. 10c, d, e). In the background sediment, the ratio rAP/LCF allows reconstructing the long-term evolution of the vegetation cover within a watershed, using the respective contribution of soil (rAP) and litter (LCF) material in the terrestrial organic matter fluxes delivered to the lake by runoff on topsoil layers (Di Giovanni et al., 2000; Simonneau et al., 2013), whereas in flood events values of the ratio rAP/LCF can reflect the source areas of material eroded during a flood event. The significance of the rAP/LCF ratio in flood SEs is further supported by the shape of the S2 curves from flood SE samples (see Sect. 4.3., unimodal or bimodal S2 curves) which can be typical of grassland or forest soils (Fig. 10d).

5.4.1 During the early Holocene: from 10 000 to 8000 cal. yr BP

Between 10 000 and 8000 cal. yr BP, the ratio rAP/LCF from background sediment fluctuated (Fig. 10c) resulting from variations in litter and soil particle supply. HI values (Fig. 10e) show exactly the same trend. This pattern suggests that the soils present through the drainage basin of Lake Ledro were not stabilized yet and that runoff processes could affect grassland areas (essentially delivering rAP particles) as well as forested ones (essentially delivering LCF particles). This is in agreement with Magny et al. (2012) and Joannin et al. (2013) who documented the progressive reforestation of the area during this period. Around 8200–8000 cal. yr BP, high values of the rAP/LCF ratio are measured in background sediment samples. This indicates a period of enhanced grassland soil erosion, which matches a cold and wet period such as the 8.2 event, frequently documented in western Europe (von Granfenstein et al., 1999) and notably at Lake Ledro (Magny et al., 2012).

In flood events the ratio rAP/LCF is always high (Fig. 10c), suggesting that soil particles (rAP) are essentially exported. S2 curves from the flood events dated from this period are unimodal and symmetric (Fig. 10d) and therefore typical of runoff on superficial layers from grassland soil, suggesting that high altitude areas (or still not reforested ones) were preferentially affected by flash floods during the early Holocene.

5.4.2 During the mid-Holocene: from 8000 to 4200 cal. yr BP

Between 8000 and 4200 cal. yr BP, the ratio rAP/LCF from background sediment is low (Fig. 10c), indicating that litter material is preferentially exported compared to soil particles by runoff processes. This suggests (i) that the catchment area of Lake Ledro was essentially forested during this period, which is in agreement with Joannin et al. (2013), and (ii) that this reforestation stabilized the soils. The lower erosion rate documented here is further supported by the lower lake levels documented by Magny et al. (2009, 2012) at Lake Ledro during this period. Indeed, these conditions resulted from a drier and warmer climate, which among other things limited the runoff. HI values (Fig. 10e) are higher than 300 mgHC g^{-1} TOC over this period, reflecting both the lower soil supply into lake sediment and the higher contribution of lacustrine algal production (correlation between HI and algal productivity: $R = 0.67$, $p < 0.001$), certainly favoured by the warmer climate.

In flood SEs, the ratio rAP/LCF is high (Fig. 10c) and the shape of the S2 curve is unimodal and symmetric (Fig. 10d) during this second period. This indicates that during the mid-Holocene, the organic material exported during flood events is still essentially made of soil particles from grassland (high-elevated) areas.
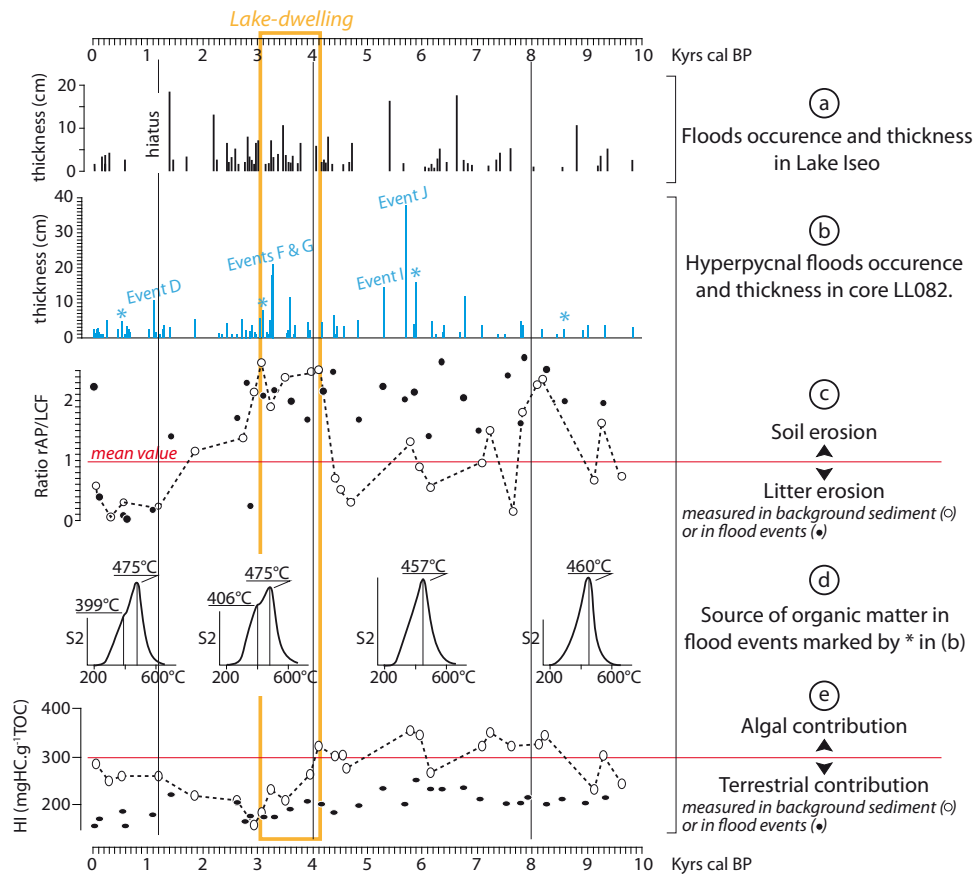
Fig. 10. Chronology and thickness of Holocene hyperpycnal flood events in the southern Alps documented by Lauterbach et al. (2012) in Lake Iseo (**a**), and higher than 1 cm thick in core LL082 from Lake Ledro (**b**), the evolution of the source of material remobilized by runoff processes within Lake Ledro watershed is given in (**c**) and calculated by the ratio of rAP on LCF for background sediment (white dots) and flood sedimentary events (black dots) in core LL082. The S2 curves from flood deposits (marked by a star in **b**) are given in (**d**) and indicate the type of organic matter present in these events as discussed in the text. The hydrogen index (HI) given in (**e**) is measured in background sediment (white dots) and flood sedimentary events (black dots) from core LL082.

5.5 During the late Holocene: from 4200 to 3100 cal. yr BP

Between 4200 and 3100 cal. yr BP, the high rAP/LCF ratio in Lake Ledro background sediment reflects enhanced soil erosion from non-forested areas topsoils. This is further supported by the HI values measured in background sediment which decrease below 300 mgHC g^{-1}TOC (Fig. 10e) suggesting higher terrestrial contribution into lake sediment by runoff processes (correlation between HI and soil particles: $R = 0.71$, $p = 0.03$). Moreover, this higher terrestrial supply is contemporaneous to the increase of lacustrine sediment magnetic susceptibility interpreted by Vannière et al. (2013) as the result of higher soil erosion. These results probably reflect the cumulative effects of (i) the climate shift to wetter conditions (Magny et al., 2012) and thereby higher runoff and of (ii) the human-induced land openness documented by Joannin et al. (2013). Indeed, this time interval is matching a period of well-documented human settlements along the shores of several lakes from the southern Alps, including

Lake Ledro (Magny et al., 2009, 2012; Fig. 2b). Bronze Age in Italy is particularly known for a sustained increase in human impact (Cremaschi et al., 2006). These human-induced soil destabilizations could favour the soil erosion under wetter climatic conditions.

In flood SEs, a high rAP/LCF ratio is measured (Fig. 10c) suggesting that the material from open landscapes was remobilized. However, the shape of the S2 curve from flood deposits is bimodal and dissymmetric (Fig. 10d) and therefore typical of forested areas. These two results suggest that the superficial layers from former forested soils were preferentially destabilized and eroded during the Bronze Age flash flood events. Both the increase of the mean flood frequency from 4 to 9.2 events per millennia (Fig. 10b) and the increasing thickness of the floods recorded in the central basin of Lake Ledro during this period (events F and G for example, Fig. 10b) may thereby have resulted from a combination of more humid climate conditions and human-induced soil destabilization and erosion.

During the late Holocene: from 3100 to present-day

During the time interval 3100–1200 cal. yr BP, the ratio rAP/LCF from background sediment and flood deposits dropping progressively (Fig. 10c), suggesting reduced soil particle erosion over the catchment area, which is in agreement with the slight drop in zirconium influx coming from soil erosion documented by Vannière et al. (2013). This reduction of erosion processes could indicate a certain stabilization of the soil within the drainage basin or changes in human land use. After 1200 cal. yr BP, the interpretation of the ratio rAP/LCF in background sediment, however, becomes more difficult. The lower values of the ratio rAP/LCF seem to indicate that the erosion processes essentially exported litter material from forested topsoil layers (Fig. 10c). During the same time interval, Vannière et al. (2013) described higher minerogenic supply coming from soil erosion (zirconium influx) and land openness from 950 cal. yr BP. Both increase in minerogenic supply and decrease in rAP/LCF ratio in background sediment are typical of the remobilization of deeper soil layers where the rAP/LCF ratio is constant whatever the vegetation cover (Graz et al., 2010). In this case, both minerogenic and organic results suggest drastic landscape disturbances over the catchment probably associated with ploughing activities and intensive human impact that affected deeper soil layers over the last millennium.

In flood SEs, a low rAP/LCF ratio is also measured (Fig. 10c) and the shape of the S2 curve from flood deposits is bimodal and dissymmetric (Fig. 10d), which is typical of forested areas. Combined with our previous hypothesis on the background sediment signal, these two results suggest that the deeper layers from former forested soils could be destabilized and eroded during recent flood SEs. Moreover, frequent but finer hyperpycnal flood deposits are recorded during this period (Fig. 10b). They may result from an anthropogenic reorganization of the drainage basin. The last hyperpycnal flood deposit recorded in our sediment cores is dated to AD 1920 ± 20 and is 2 cm thick. It is interesting to note that Lake Ledro does not record any other hyperpycnal flood after this date. This suggests either a primary climate signature (Pfister, 2009) or that regulating activities during hydropower production since AD 1929 can modify the temperature of the water column and maybe prevent the generation of hyperpycnal floods, or more probably that recent human infrastructure on river corrections in the catchment area have been very efficient in reducing the impact of flash flood events on lacustrine environments.

6 Conclusions

In Lake Ledro, the combination of high-resolution seismic profiling with physical and organic analyses of sediment cores and soil and riverbed samples allows (i) characterizing the sensitivity of Holocene lacustrine sedimentation to changes in vegetation cover within the drainage basin and (ii) distinguishing the origins of the contrasted sedimentary events which regularly interrupted the background sedimentation. Up to 73 catastrophic hyperpycnal flood deposits (> 1 cm) resulting from the combination of heavy rainfalls with snowmelt have especially been discriminated from 14 subaquatic mass-wasting deposits.

Distal mass-flow deposits in the central basin of Lake Ledro are generally associated with numerous coeval mass-movements along the steep slopes of the basin affecting not only deltaic environments. Half of these coeval mass-movements matching chronologically either historical regional earthquakes (in AD 2004, 1901, 1891 and 1117 or 1046) or coeval mass-movements in nearby Lake Iseo documented by Lauterbach et al. (2012) around 2525 ± 110 and 4490 ± 110 cal. yr BP, providing new evidence that the Southern Italian Alps have been frequently affected by large regional earthquakes. Similar coeval mass-movements dated around 3350 ± 80, 3815 ± 85, 5890 ± 90, 7190 ± 130, 9185 ± 85 and 11 495 ± 340 cal. yr BP are supposed to be related to previously undocumented (and eventually more local) earthquakes.

The long-term evolution of the vegetation cover in the drainage basin of Lake Ledro has been deduced from the respective contributions of soil and litter fluxes delivered to the lake by runoff in background sediments. During the first half of the Holocene, the drainage basin was forested and hyperpycnal floods essentially affected grassland areas. Inversely, after around 5000–4500 cal. yr BP climate variability favoured the development of flash floods after the snow season and the intensification of human activities increased soil erosion, especially between 4000 and 3100 cal. yr BP. Enhanced occurrence of natural hazards such as earthquakes and flash floods during this period may have, in addition, contributed to the decline of the lake-dwelling at Lake Ledro. Our results also suggest that over the last millennium changes in human land use, such as ploughing activities, may have affected the deeper soil layers.

This study highlights that, since present-day climate or modern river corrections apparently succeeded in diminishing the development of hyperpycnal flood events in Lake Ledro, land use combined with future climate changes may have irreversible consequences on soil erosion and on the pedogenesis preserved until now.

References

Ariztegui, D., Chondrogianni, C., Lami, A., Guilizzoni, P., and Lafargue, E.: Lacustrine organic matter and the Holocene paleoenvironmental record of Lake Albano (central Italy), J. Paleolimnol., 26, 283–292, 2001.

Arnaud, F., Revel, M., Chapron, E., Desmet, M., and Tribovillard, N.: 7200 years of Rhone river flooding activity in Lake Le Bourget, France: a high-resolution sediment record of NW Alps hydrology, Holocene, 15, 420–428, 2005.

Barredo, J. I.: Major flood disaster in Europe: 1950–2005, Nat. Hazards, 42, 125–148, 2007.

Behar, F., Beaumont, V., and De B. Penteado, H. L.: Rock-Eval 6 Technology: performances and Developments, Oil Gas Sci. Technol., 56, 111–134, 2001.

Beniston, M., Stephenson, D. B., Christensen, O. B., Ferro, C. A. T., Frei, C., Goyette, S., Halsnaes, K., Holt, T., Jylhä, K., Koffi, B., Palutikol, J., Schöll, R., Semmler, T., and Woth, K.: Future extreme events in European climate: an exploration of regional climate model projections, Climatic Change, 81, 71–95, 2007.

Beug, H. J.: Untersuchungen zur spätglazialen Vegetationsgeschichte im Gardaseegebiet unter besonderer Berücksichtigung der mediterranen Arten, Flora, 154, 401–440, 1964.

Bøe, A. G., Dahl, S. O., Lie, Ø., and Nesje, A.: Holocene river floods in the upper Glomma catchment, southern Norway: a high-resolution multiproxy record from lacustrine sediments, Holocene, 16, 445–455, 2006.

Bollettinari, G., Picotti, V., Cantelli, L., Castellarin, A., Trombetta, G., and Claps, M.: Carta geologica d'Italia – Riva del Garda, Foglio 080 della carta 1 : 50.000 dell'I.G.M., 2005.

Bornhold, B. D., Ren, P., and Prior, D. B.: High-frequency turbidity currents in British Columbia fjords, Geo-Mar. Lett., 14, 238–243, 1994.

Brauer, A., Dulski, P., Mangili, C., Mingram, J., and Liu, J.: The potential of varves in high-resolution paleolimnological studies, PAGES News, 17, 96–98, 2008.

Buma, J. and Dehn, M.: A method for predicting the impact of climate change on slope stability, Environ. Geol., 35, 190–196, 1998.

Calvert, S. E.: Beware intercepts: interpreting compositional ratios in multi-component sediments and sedimentary rocks, Org. Geochem., 35, 981–987, 2004.

Cerdà, A.: The influence of geomorphological position and vegetation cover on the erosional and hydrological processes on a Mediterranean hillslope, Hydrol. Process., 12, 661–671, 1998.

Cerdà, A.: Parent Material and Vegetation Affect Soil Erosion in Eastern Spain, Soil Sci. Soc. Am. J., 63, 362–368, 1999.

Chapron, E., Beck, C., Pourchet, M., and Deconninck, J. F.: 1822 earthquake-triggered homogenite in Lake Le Bourget (NW Alps), Terra Nova, 11, 86–92, 1999.

Chapron, E., Desmet, M., De Putter, T., Loutre, M. F., Beck, C., and Deconinck, J. F.: Climatic variability in the northwestern Alps, France, as evidence by 600 years of terrigenous sedimentation in Lake Le Bourget, Holocene, 12, 177–185, 2002.

Chapron, E., Arnaud, F., Noël, H., Revel, M., Desmet, M., and Perdereau, L.: Rhone River flood deposits in Lake Le Bourget: a proxy for Holocene environmental changes in the NW Alps, France, Boreas, 34, 404–416, 2005.

Chapron, E., Juvigné, E., Mulsow, S., Ariztegui, D., Magand, O., Bertrand, S., Pino, M., and Chapron, O.: Recent clastic sedimentation processes in Lake Puyehue (Chilean Lake District, 40.5° S), Sediment. Geol., 201, 365–385, 2007.

Christensen, J. H. and Christensen, O. B.: Climate modelling: Severe summertime flooding in Europe, Nature, 421, 805–806, 2003.

Combaz, A.: Les palynofaciès, Revue de Micropaléontologie, 7, 205–218, 1964.

Copard, Y., Di Giovanni, C., Martaud, T., Albéric, P., and Olivier, J. E.: Using Rock-Eval 6 pyrolysis for tracking fossil organic carbon in modern environments: implications for the roles of erosion and weathering, Earth Surf. Proc. Land., 31, 135–153, 2006.

Cremaschi, M., Pizzi, C., and Valsecchi, V.: Water management and land use in the terramare and a possible climatic co-factor in their abandonment: The case study of the terramara of Poviglio Santa Rosa (northern Italy), Quaternary Int., 151, 87–98, 2006.

Czymzik, M., Brauer, A., Dulski, P., Plessen, B., Naumann, R., von Grafeinstein, U., and Scheffler, R.: Orbital and solar forcing of shifts in Mid- to Late Holocene flood intensity from varved sediments of pre-alpine Lake Ammersee (southern Germany), Quaternary Sci. Rev., 61, 96–110, 2010.

Dearing, J. A.: Climate-human-environment interactions: resolving our past, Clim. Past, 2, 187–203, doi:10.5194/cp-2-187-2006, 2006.

Dearing, J. A., Battarbee, R. W., Dikau, R., Larocque, I., and Oldfield, F.: Human-environment interactions: learning from the past, Reg. Environ. Change, 6, 1–16, 2006.

Debret, M., Chapron, E., Desmet, M., Rolland-Revel, M., Magand, O., Trentesaux, A., Bout-Roumazeille, V., Nomade, J., and Arnaud, F.: North western Alps Holocene paleohydrology recorded by flooding activity in Lake Le Bourget, France, Quaternary Sci. Rev., 29, 2185–2200, 2010.

De Ploey, J.: Bassins versants ravinés: analyses et prévisions selon le modèle Es, Bulletin de la Société géographique de Liège, 27, 69–76, 1991.

De Ploey, J., Moeyersons, J., and Goosens, D.: The De Ploey erosional susceptibility model for catchments, Es, Catena, 25, 269–314, 1995.

Di Giovanni, C., Disnar, J. R., Campy, M., Bichet, V., and Guillet, B.: Geochemical characterization of soil organic matter and variability of a post glacial detrital organic supply (Chaillexon lake, France), Earth Surf. Proc. Land., 23, 1057–1069, 1998.

Di Giovanni, C., Disnar, J. R., Bichet, V., and Campy, M.: Seasonal variability and threshold effects of the organic detrital sedimentation in lakes: imbalances between organic records and climatic fluctuations (Chaillexon basin, Doubs, France), B. Soc. Geol. Fr., 171, 533–544, 2000.

Disnar, J. R., Guillet, B., Keravis, D., Di Giovanni, C., and Sebag, D.: Soil organic matter (SOM) characterization by Rock-Eval pyrolysis: scope and limitations, Org. Geochem., 34, 327–343, 2003.

Duchaufour, P.: Pédogenèse et classification, 2nd Edn., Masson, Paris, 491 pp., 1983.

Espitalié, J., Deroo, G., and Marquis, F.: La pyrolyse Rock-Eval et ses applications. Première partie, Oil Gas Sci. Tech., 40, 563–579, 1985.

Fanetti, D., Anselmetti, F. S., Chapron, E., Sturm, M., and Vezzoli, L.: Megaturbidite deposits in the Holocene basin fill of Lake Como (Southern Alps, Italy), Palaeogeogr. Palaeocl., 259, 323–340, 2008.

Gilli, A., Anselmetti, F. S., Glur, L., and Wirth, S. B.: Lake sediments as archives of reccurrence rates and intensities of past flood events, in: Dating torrential processes on fans and cones – methods and their application for hazard and risk assessment, edited by: Michelle Schneuwly-Bollschweiler, M. S., Stoffel, M., and Rudolf-Miklau, F., Adv. Glob. Change Res., 47, 225–242, Springer, doi:10.1007/978-94-007-4336-6_15, 2013.

Girard, M. C., Walter, C., Rémy, J. C., Berthelin, J., and Morel, J. L.: Sols et environnements, 2nd Edn., Dunod, Paris, 881 pp., 2011.

Graz, Y., Di Giovanni, C., Copard, Y., Laggoun-Défarge, F., Boussafir, M., Lallier-Vergès, E., Baillif, P., Perdereau, L., and Simonneau, A.: Quantitative palynofacies analysis as a new tool to study transfers of fossil organic matter in recent terrestrial environments, Int. J. Coal Geol., 84, 49–62, 2010.

Guidoboni, E. and Comastri, A.: The "exceptional" earthquake of 3 January 1117 in the Verona area (northern Italy): A critical time review and detection of two lost earthquakes (lower Germany and Tuscany), J. Geophys. Res., 110, 1–20, 2005.

Guidoboni, E., Ferrari, G., Mariotti, D., Comastri, A., Tarabusi, G., and Valensise, G.: Catalogue of strong earthquakes in Italy 461B.C.-1997 and Mediterranean area 760 B.C.–1500, available at: http://storing.ingv.it/cfti4med/ (last access: 15 January 2011), 2007.

Jacob, J., Disnar, J. R., Boussafir, M., Sifeddine, A., Turcq, B., and Spadano Albuquerque, A. L.: Major environmental changes recorded by lacustrine sedimentary organic matter since the last glacial maximum near the equator (Lagoa do Caçó, NE Brazil), Palaeogeogr. Palaeocl., 205, 183–197, 2004.

Jacob, J., Disnar, J. R., Arnaud, F., Gauthier, E., Billaud, Y., Chapron, E., and Bardoux, G.: Impacts of new agricultural practices on soil erosion during the Bronze Age in the French Prealps, Holocene, 19, 241–249, 2009.

Joannin, S., Vannière, B., Galop, D., Magny, M., Gilli, A., Chapron, E., Wirth, S., Anselmetti, F. S., and Desmet, M.: Holocene vegetation and climate changes in the Central Mediterranean at Lake Ledro (Trentino, Italy), Clim. Past Discuss., in press, 2013.

Knox, J. C.: Sensitivity of modern and Holocene floods to climate change, Quaternary Sci. Rev., 19, 439–457, 2000.

Lambert, A. and Giovanoli, F.: Records of riverborne turbidity currents and indications of slope failures in the Rhone delta of Lake Geneva, Limnol. Oceanogr., 33, 458–168, 1988.

Lauterbach, S., Chapron, E., Brauer, A., Hüls, M., Gilli, A., Arnaud, F., Piccin, A., Nomade, J., Desmet, M., von Grafenstein, U.: A sedimentary record of Holocene surface runoff events and earthquake activity from Lake Iseo (Southern Alps, Italy), Holocene, 22, 749–760, 2012.

Le Bissonnais, Y., Montier, C., Jamagne, M., Daroussin, J., and King, D.: Mapping erosion risk for cultivated soil in France, Catena, 46, 207–220, 2001.

Lotter, A. F. and Lemcke, G.: Methods for preparing and counting biochemical varves, Boreas, 28, 243–252, 1999.

Magny, M., Galop, D., Bellintani, P., Desmet, M., Didier, J., Haas, J. N., Martinelli, N., Pedrotti, A., Scandolari, R., Stock, A., and Vannière, B.: Late-Holocene climatic variability south of the Alps as recorded by lake-level fluctuations at Lake Ledro, Trentino, Italy, Holocene, 19, 575–589, 2009.

Magny, M., Arnaud, F., Holzhauser, H., Chapron, E., Debret, M., Desmet, M., Leroux, A., Millet, L., Revel, M., and Vannière, B.: Solar and proxy-sensitivity imprints on paleohydrological records for the last millennium in west-central Europe, Quaternary Res., 73, 173–179, 2010.

Magny, M., Joannin, S., Galop, D., Vannière, B., Haas, J. N., Basseti, M., Bellintani, P., Scandolari, R., Desmet, M.: Holocene paleohydrological changes in the northern Mediterranean borderlands as reflected by the lake-level record of Lake Ledro, north-eastern Italy, Quaternary Res., 77, 382–396, doi:10.1016/j.yqres.2012.01.005, 2012.

Marchi, L., Borga, M., Preciso, E., and Gaume, E.: Characterization of selected extreme flash floods in Europe and implications for flood risk management, J. Hydrol., 394, 118–133, 2010.

Mudelsee, M., Börngen, M., Tetzlaff, G., and Grünewald, U.: No upward trends in the occurrence of extreme floods in central Europe, Nature, 425, 166–169, 2003.

Mulder, T. and Alexander, J.: The physical character of subaqueous sedimentary density flows and their deposits, Sedimentology, 48, 269–299, 2001.

Mulder, T. and Chapron, E.: Flood deposits in continental and marine environments: character and significance, in: Sediment transfer from shelf to deep water — Revisiting the delivery system, AAPG Studies in Geology, 61, edited by: Slatt, R. M. and Zavala, C., 1–30, 2011.

Mulder, T. and Cochonat, P.: Classification of offshore mass movements, J. Sediment. Res., 66, 43–57, 1996.

Mulder, T., Syvitski, J. P. M., Migeon, S. Faugères, J. C., and Savoye, B.: Marine hyperpycnal flows: initiation, behavior and related deposits. A review, Mar. Petrol. Geol., 20, 861–882, 2003.

Noël, H., Garbolino, E., Brauer, A., Lallier-Vergès, E., de Beaulieu, J. L., and Disnar, J. R.: Human impact and soil erosion during the last 5000 yrs as recored in lacustrine sedimentary organic matter at Lac d'Annecy, the French Alps, J. Paleolimnol., 25, 229–244, 2001.

Ollesch, G., Kistner, I., Meissner, R., and Lindenschmidt, K. E.: Modelling of snowmelt erosion and sediment yield in a small low-mountain catchment in Germany, Catena, 68, 131–176, 2006.

Pfister, C.: Die "Katastrophenlücke" des 20. Jahrhunderts und der Verlust traditionalen Risikobewusstseins, GAIA, 18, 239–246, 2009.

Raclot, D. and Albergel, J.: Runoff and water erosion modelling using WEPP on a Mediterranean cultivated catchment, Phys. Chem. Earth, 31, 1038–1047, 2006.

Ramanampisoa, L. and Disnar, J. R.: Primary control of paleoproduction on organic matter preservation and accumulation in the Kimmeridge rocks of Yorkshire (UK), Org. Geochem., 21, 1153–1167, 1994.

Reimer, P. J., Baillie, M. G. L., Bard, E., Bayliss, A., Beck, J. W., Blackwell, P. G., Bronk Ramsey, C., Buck, C. E., Burr, G. S., Edwards, R. L., Friedrich, M., Grootes, P. M., Guilderson, T. P., Hajdas, I., Heaton, T. J., Hogg, A. G., Hughen, K. A., Kaiser, K. F., Kromer, B., McCormac, F. G., Manning, S. W., Reimer, R. W., Richards, D. A., Southon, J. R., Talamo, S., Turney, C. S. M., van der Plicht, J., and Weyhenmeyer, C. E.: IntCal09 and Marine09 radiocarbon age calibration curves, 0–50,000 years cal BP, Radiocarbon, 51, 1111–1150, 2009.

Schnellmann, M., Anselmetti, F. S., Giardini, D., McKenzie, J. A., and Ward, S. N.: Prehistoric earthquake history revealed by lacustrine slump deposits, Geology, 30, 1131–1134, 2002.

Sebag, D., Disnar, J. R., Guillet, B., Di Giovanni, C., Verrecchia, E. P., and Durand, A.: Monitoring organic matter dynamics in soil profiles by "Rock-Eval pyrolysis": bulk characterization and quatification of degradation, Eur. J. Soil Sci., 57, 344–355, 2005.

Sebag, D., Copard, Y., Di Giovanni, C., Durand, A., Laignel, B., Ogier, S., and Lallier-Vergès, E.: Palynofacies as useful tool to study origins and transfers of particulate organic matter in recent terrestrial environments: Synopsis and prospects, Earth-Sci. Rev., 79, 241–259, 2006.

Sifeddine, A., Bertrand, P., Lallier-Vergès, E., and Patience, A. J.: Lacustrine organic fluxes and palaeoclimatic variations during the last 15 ka: Lac du Bouchet (Massif Central, France), Quaternary Sci. Rev., 15, 203–211, 1996.

Simonneau, A., Doyen, E., Chapron, E., Millet, L., Vannière, B., Di Giovanni, C., Bossard, N., Tachikawa, K., Bard, E., Albéric, P., Desmet, M., Roux, G., Lajeunesse, P., Berger, J.-F., and Arnaud, F.: Holocene land-use evolution and associated soil erosion in the French Prealps inferred from Lake Paladru sediments and archaeological evidences, J. Archaeol. Sci., 40, 1636–1645, 2013.

Souchère, V., Cerdan, O., Ludwig, B., Le Bissonnais, Y., Couturier, A., and Papy, F.: Modelling ephemeral gully erosion in small cultivated catchments, Catena, 50, 489–505, 2003.

Stewart, M. M., Grosjean, M., Kuglitsch, F. G., Nussbaumer, S. U., and von Gunten, L.: Reconstructions of late Holocene paleofloods and glacier length changes in the Upper Engadine, Switzerland (ca. 1450 BC–AD 420), Palaeogeogr. Palaeocl., 311, 215–223, 2011.

St-Onge, G., Mulder, T., Piper, D. J. W., Hillaire-Marcel, C., and Stoner, J. S.: Earthquake and flood-induced turbidites in the Saguenay Fjord (Québec): a Holocene paleoseismicity record, Quaternary Sci. Rev., 23, 283–294, 2004.

St-Onge, G., Chapron, E., Mulsow, S., Salas, M., Viel, M., Debret, M., Foucher, A., Mulder, T., Winiarski, T., Desmet, M., Costa, P. J. M., Ghaleb, B., Jaouen, A., and Locat, J.: Comparison of earthquake-triggered turbidites from the Saguenay (Eastern Canada) and Reloncavi (Chilean margin) Fjords: Implications for paleoseismicity and sedimentology, Sediment. Geol., 243–244, 89–107, 2012.

Talbot, M. R. and Livingstone, D. A.: Hydrogen index and carbon isotopes of lacustrine organic matter as lake level indicators, Palaeogeogr. Palaeocl., 70, 121–137, 1989.

Tanasienko, A. A., Yakutina, O. P., and Chumbaev, A. S.: Snowmelt runoff parameters and geochemical migration of elements in the dissected forest-steppe of West Siberia, Catena, 78, 122–128, 2009.

Tanasienko, A. A., Yakutina, O. P., and Chumbaev, A. S.: Effect of snow amount on runoff, soil loss and suspended sediment during periods of snowmelt in southern West Siberia, Catena, 87, 45–51, 2011.

Tropeano, D. and Turconi, L.: Using Historical Documents for Landslide, Debris Flow and Stream Flood Prevention, Applications in Northern Italy, Nat. Hazards, 31, 663–679, 2004.

Tyson, R. V.: Sedimentary Organic Matter: Organic Facies and Palynofacies, Chapman and Hall, London, 615 pp., 1995.

Vannière, B., Wirth, S., Simonneau, A., Gilli, A., Joannin, S., Chapron, E., Anselmetti, F. S., and Magny, M.: Orbital and solar control versus human activities impact on European "Flooding Increase Periods" (the record of Lake Ledro, Northern Italy), Clim. Past Discuss., accepted, 2013.

von Grafenstein, U., Erlenkeuser, H., Brauer, A., Jouzel, J., and Johnsen, S. J.: A Mid-European Decadal Isotope-CLimate Record from 15,500 to 5000 Years B.P., Science, 284, 1654–1657, 1999.

Wanner, H., Solomina, O., Grosjean, M., Ritz, S. P., and Jetel, M.: Struture and origin of Holocene cold events, Quaternary Sci. Rev., 30, 3109–3123, 2011.

Wirth, S. B., Girardclos, S., Rellstab, C., and Anselmetti, F. S.: The sedimentary response to a pioneer geo-engineering project: Tracking the Kander River deviation in the sediments of Lake Thun (Switzerland), Sedimentology, 58, 1737–1761, 2011.

Wirth, S. B., Gilli, A., Glur, L., Anselmetti, F. S., Ariztegui, D., Simonneau, A., Chapron, E., Vannière, B., and Magny, M.: Reconstructing the seasonality of late Holocene flood events using varved lake sediments of Lake Ledro (Southern Alps, Italy), 3rd PAGES Varves Working Group Workshop, Manderscheid, Germany, 2012.

Wohl, E. E.: Inland Flood Hazards: Human, Riparian, and Aquatic Communities, Cambridge University Press, 2000.